Letter

Polarization-resolved electron spin resonance in a two-dimensional electron system

D. A. Khudaiberdiev , A. Shuvaev , A. V. Shchepetilnikov , V. M. Muravev, M. M. Glazov , C. Reichl, J. W. Wegscheider, A. Pimenov , and I. V. Kukushkin

"Institute of Solid State Physics, Technische Universität Wien, 1040 Vienna, Austria

"Osipyan Institute of Solid State Physics, RAS, Chernogolovka 142432, Russia

"Institute, St. Petersburg 194021, Russia

"Laboratory for Solid State Physics, ETH Zurich, CH-8093 Zurich, Switzerland

"Quantum Center, ETH Zurich, CH-8093 Zurich, Switzerland

(Received 11 January 2025; revised 2 May 2025; accepted 2 September 2025; published 1 October 2025)

We report on polarization-resolved electron spin resonance (ESR) in a two-dimensional electron system in AlAs quantum wells. The transmission spectra in the subterahertz frequency range reveals unusual behavior as a function of the light polarization and of experimental geometry. In the Faraday geometry, the excitation conditions for spin resonance are reversed compared with the cyclotron resonance, while in the Voigt geometry the absorption exhibits a twofold dependence on the azimuthal angle of an in-plane static magnetic field. These results contradict a pure magnetic nature of ESR in AlAs quantum wells, revealing a dominating Dresselhaus spin-orbit coupling as a microscopic mechanism of the electric-dipole absorption. A theoretical model that includes an inversion asymmetry and the spin-orbit coupling successfully explains the experimental observations.

DOI: 10.1103/4lyv-jvq5

An electron ensemble with a nonzero spin degree of freedom represents a quantum object that may be coupled to classical electromagnetic radiation. This interaction can lead to resonant radiation absorption and spin excitation, known as electron spin resonance (ESR). The spin-light interaction for a free electron can be well understood using the semiclassical Bloch formalism [1]. Within the quantum approach, the ESR is typically described as a result of magnetodipole transitions between Zeeman-split spin sublevels. In most practical cases, such as conduction electrons in solids, the presence of strong internal electric fields makes the task more complex. These fields enable the spin-orbit interaction (SOI), which is the coupling of electron spin to its kinetic motion [2-4]. The AC electric field of light modulates the electron wave vector, leading to an effective oscillating SOI-induced magnetic field that causes spin rotation [5,6]. Electron spin resonance excited by such mechanism is called electric-dipole spin resonance (EDSR). The ability to manipulate spins using an electric field is of great importance for electronic applications. It enables precise control of individual spins at the nanoscale, bridging conventional electronics and spintronics [7–11]. Additionally, the spin-light coupling in the quasioptical scheme can be effectively tuned and boosted by using standard resonators where the electric field is accumulated and enhanced [12–15].

An electric-dipole contribution to the spin excitation exists for conduction electrons in bulk crystals with strong SOI [16–18] and also for localized spins in quantum dots [8]. Several attempts have been made to experimentally investigate

Published by the American Physical Society under the terms of the Creative Commons Attribution 4.0 International license. Further distribution of this work must maintain attribution to the author(s) and the published article's title, journal citation, and DOI.

the physical nature of ESR in semiconductor heterostructures containing two-dimensional (2D) electrons [19-22]. Surprisingly, these studies yielded controversial results. For example, ESR has a magnetic-dipole origin in a GaAs quantum well with strong spin-orbit coupling [19] and, counterintuitively, it exhibits an electric-dipole nature in silicon quantum wells [21]—an electron system with two orders of magnitude weaker SOI. A significant challenge in these experiments is the difficulty of maintaining a pure polarization state of electromagnetic radiation in the microwave and terahertz (THz) frequency ranges. For example, in Refs. [19,22], the relatively narrow Hall-bar and metallic contacts may have introduced distortions to the electric and magnetic fields of the incident wave. Similarly, a complex field distribution inside a microwave resonator with a sample inside [20,21] may also complicate the analysis.

In this work, we investigate the polarization-dependent terahertz absorption of the spin resonance in an AlAs-based two-dimensional electron system. We employ a quasioptical technique [23] with large samples to ensure a high degree of polarization purity leading to strong sensitivity of ESR to the polarization of light. The obtained results provide strong evidence that the spin resonance in AlAs quantum wells is electric-dipole active and originates from the Dresselhaus spin-orbit interaction, which is a result of the bulk inversion asymmetry (BIA).

The samples under study were fabricated from AlAs/Al_xGa_{1-x}As (x = 0.46) heterostructures grown along the [001] direction via molecular beam epitaxy. The heterostructures contained a 4.5 nm AlAs quantum well (QW) hosting a two-dimensional electron system (2DES); see Ref. [24] for details. The bottom conduction band of bulk AlAs material has three energy-degenerate valleys located at the X points of the Brillouin zone and aligned along the [100],

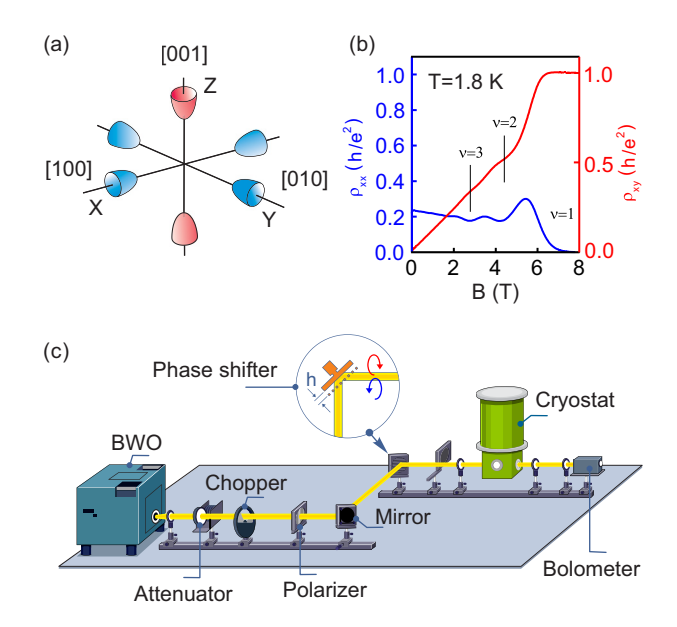


FIG. 1. (a) Fermi surface of the bulk AlAs. Electrons in a 4.5 nm quantum well occupy the Z valley, marked by red color. (b) Results of the transport measurements at T=1.8 K. Left blue axis shows longitudinal resistivity $\rho_{xx}(B)$, whereas the right red axis corresponds to Hall resistivity $\rho_{xy}(B)$. (c) Schematic diagram of the quasioptical setup in the sub-THz range.

[010], and [001] crystallographic directions, respectively [Fig. 1(a)]. The corresponding elliptical Fermi contours are characterized by a heavy longitudinal mass $m_1 = 1.1 m_0$ and a light transverse mass $m_{\rm tr} = 0.2 \, m_0$, where m_0 is the free electron mass [24]. Quantum confinement along the [001] direction favors the occupation of the Z valley by electrons with isotropic mass in the QW plane, as confirmed by the optical [25], magnetotransport [26], and cyclotron resonance (CR) spectroscopy [27,28]. Standard indium contacts to the 2DES were formed along the sample boundary in the van der Pauw geometry. The contacts were placed well outside the diaphragm such as not to affect the polarization state of the radiation. This fact has been further confirmed by the strong polarization sensitivity of the cyclotron resonance. Typical low-temperature electron density of $n_s = 2.05 \times 10^{11} \, \text{cm}^{-2}$ and mobility of $\mu = 5 \times 10^3 \text{ cm}^2/(\text{V s})$ have been obtained from the transport measurements [Fig. 1(b)].

An experimental setup of the present experiment is depicted in Fig. 1(c). A 8×8 mm² sample is mounted on a sample holder with a 6 mm diaphragm at the location of the sample. The entire arrangement is oriented in the Faraday (field out of plane) or Voigt (field in plane) geometries inside an optical cryostat, with a split-coil magnet providing the field up to ±8 T. The cryostat is equipped with 100 μ m thick mylar inner and outer windows, where the outer openings are covered with black polyethylene foil to block the visible light. The monochromatic radiation incident perpendicular to the sample surface is generated by backward-wave oscillators operating in the frequency range of 50–600 GHz [23]. The linear polarization of the electromagnetic wave is set by wire-grid polarizers. Circular polarization is generated by the phase shifter, which is equivalent to a tunable $\lambda/4$ plate

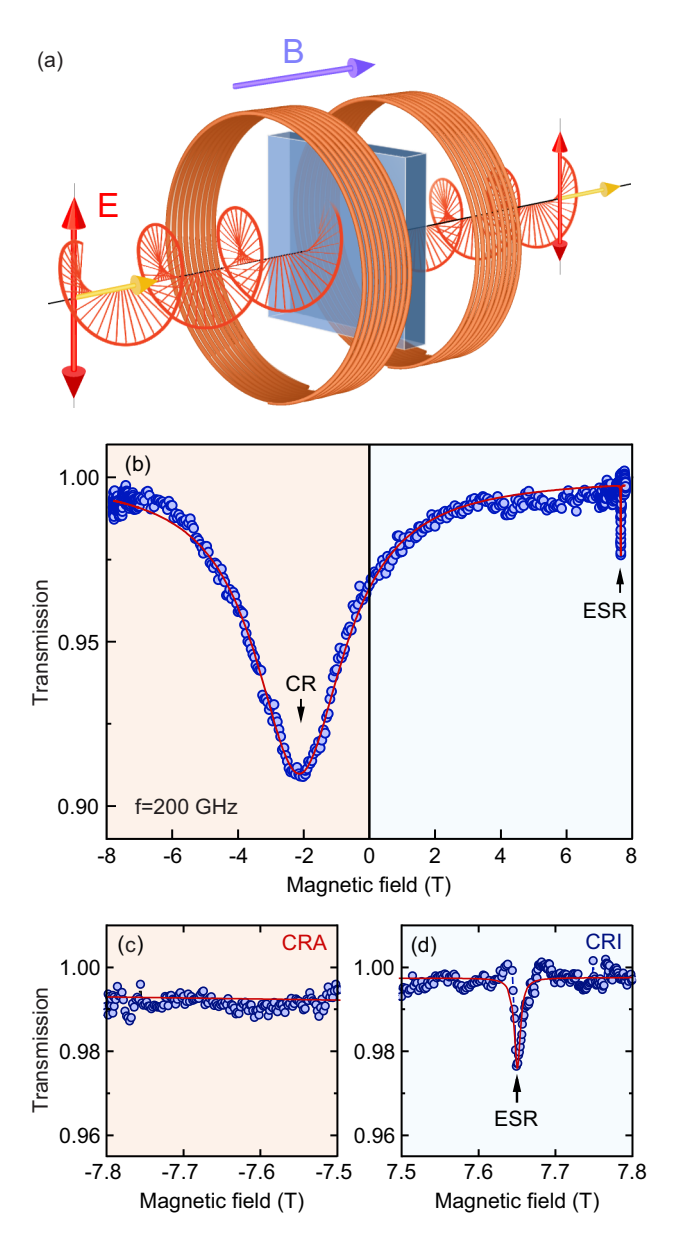


FIG. 2. (a) Configuration of quasioptical experiments in Faraday geometry with circular polarization. (b) Transmission through the sample as a function of magnetic field at $f=200~\mathrm{GHz}$. Both cyclotron resonance (CR) and electron-spin resonance (ESR) are observed simultaneously in the transmission but for opposite sign of the magnetic field. Enlarged transmission curves for the cyclotron-resonance active (CRA) and inactive (CRI) regime are given in (c) and (d), respectively.

(see Ref. [29] for more details). The radiation is directed into the cryostat by the system of mirrors and lenses. The signal transmitted through the sample is modulated by a chopper at a frequency of 23 Hz and detected by a helium-cooled bolometer using a lock-in detection scheme referenced to the chopper frequency. All measurements are done at the base sample temperature of $T=1.8~\rm K$.

The first set of experiments was carried out in the Faraday geometry with magnetic field applied parallel to the propagation direction of the THz light [Fig. 2(a)]. Figure 2(b) shows the transmission as a function of the magnetic field measured

at a fixed frequency f = 200 GHz for circularly polarized radiation. The frequency corresponds to a Fabry-Pérot maximum of the substrate transmission to eliminate the influence of the dielectric substrate [30]. For negative magnetic fields, a CR is clearly observed. The CR frequency, $\omega_c = eB/m_c c$, with e being the electron charge, yields an effective cyclotron mass of electrons $m_c = 0.27 m_0$ close to the value of the transverse mass $m_{\rm tr}$ expected in such structures. It is consistent with previous studies of narrow AlAs quantum wells [25–28] and confirms that electrons occupy a single Z valley. The CR is absent at the positive polarity of the magnetic field. The strong polarization sensitivity of the CR peak further proves that the radiation is strongly circularly polarized. Both the cyclotron resonance and the ESR show a clear Lorentz-like waveform consistent with the Drude model for dynamical conductivity in the quasiclassical approximation and for circular polarization [31].

Surprisingly, an additional narrow peak emerges in the cyclotron-resonance inactive (CRI) polarity for positive magnetic fields around B = 7.65 T [Fig. 2(d)]. Experiments show that the magnetic field position of this peak scales linearly with the frequency corresponding to the single particle spin-splitting energy $\Delta E = g_z \mu_B B$ (for more data, see Supplemental Material [32]) with the g factor $g_z = 1.88 \pm 0.01$ perfectly consistent with Landé factors measured previously in Ref. [33]. This experimental finding allows us to attribute this narrow feature to the electron spin resonance. The possibility of detecting the ESR in the quasioptical setup with a controlled polarization state of light enables a comprehensive investigation of one of the most fundamental questions in solid-state physics: How do classical electromagnetic waves interact with a quantum spin degree of freedom? The mechanism of such interaction is uncovered below on the basis of further experiments and modeling.

Importantly, the spin resonance is absent in the cyclotronresonance active (CRA) regime, Fig. 2(c). This observation directly contradicts the standard mechanism of magnetodipole induced ESR since for $g_z > 0$ the electron spin precession and the cyclotron motion occur in the same direction. This non-trivial polarization dependence indicates the excitation of the resonance through the electric dipole mechanism in the presence of Dresselhaus spin-orbit interaction, as we demonstrate below. The ESR peak has a quality factor of $Q \simeq 850$, indicating a weak coupling of the observed magnetic resonance with the electromagnetic environment and a long spin relaxation times typical of the quantum Hall effect regime at odd filling factors [34–37]. It is important to note that the filling factor of the system is v = 1 at the magnetic fields of our experiment, as shown in Fig. 1(b). Therefore, the electron system is fully spin-polarized at the magnetic field of the spin resonance B = 7.65 T.

To gain further insight into the physics of the spin-light interaction, we have performed ESR experiments with the magnetic field oriented in the plane of the quantum well and with linearly polarized THz radiation. Figure 3 shows the transmission through the sample at f=209 GHz when the magnetic field is parallel to the [100] axis (Voigt configuration) and for different angles Θ between the ac electric field \vec{E}^{AC} and static magnetic field \vec{B} , see insets. A distinct spin resonance is observed at a magnetic field of B=7.55 T.

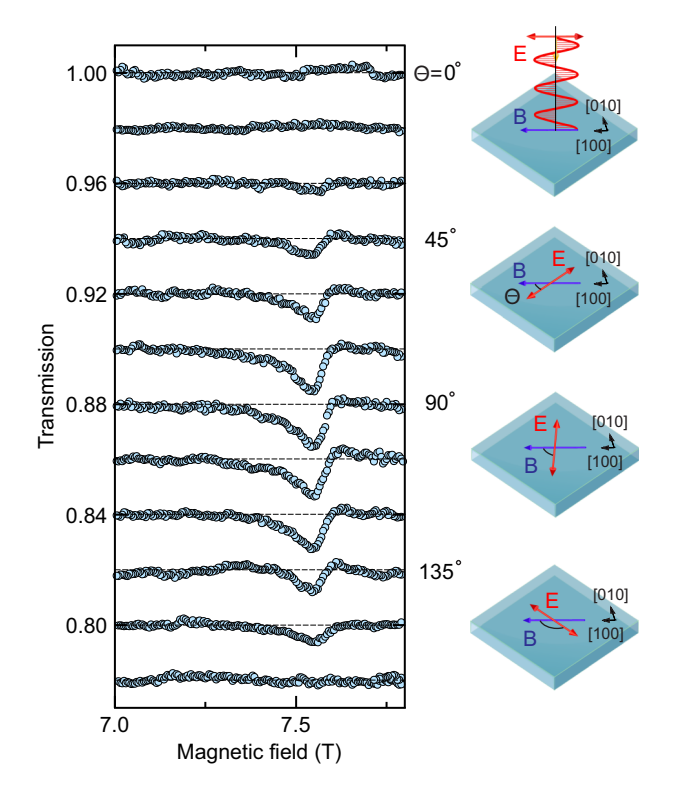


FIG. 3. Transmission through the sample at frequency f=209 GHz in the Voigt configuration, with external magnetic field oriented along the [100] axis within the sample plane. The maximum ESR amplitude occurs when the angle $\Theta=\angle\vec{B}, \vec{E}^{AC}$ is 90° , while zero signal is observed for $\Theta=0^{\circ}$. The curves are offset vertically by 0.02. The right insets sketch the configurations of the experiment.

The corresponding g factor is $g_x = 1.98 \pm 0.01$ [32]. The resonance amplitude changes with variation of Θ reaching its maximum at $\Theta = 90^{\circ}$. It is surprising that in this geometry, the ESR reaches its maximum, as the alternating magnetic field of the wave is parallel to the static magnetic field \vec{B} . In addition, we observe no resonance at $\Theta = 0^{\circ}$, where the magnetically excited resonance is expected. These experimental findings unambiguously prove that the observed electron spin resonance is not driven by the oscillating magnetic field of the wave but rather is induced by its electric field via the spin-orbit interaction in the AlAs well.

In a next step, we vary the in-plane direction of the external magnetic field. The angle α sets the orientation of the field B with respect to the [100] axis. In Fig. 4, the polar diagrams of the ESR resonance amplitudes are depicted for three different angles: $\alpha = 0^{\circ}$, $\alpha = 22.5^{\circ}$, and $\alpha = 45^{\circ}$. Each diagram was recorded by rotating the polarization of the incident electromagnetic wave while maintaining the sample in a fixed position in the cryostat. As in the previous section, the rotation angle, $\Theta = \angle \vec{B}, \vec{E}^{AC}$, is the angle between the external magnetic field and the electric field of the wave. The diagram with $\alpha = 0^{\circ}$ and therefore $\vec{B} \parallel [100]$ corresponds to the resonances in Fig. 3 discussed above. In the case of $\vec{B} \parallel [110] (\alpha = 45^{\circ})$, the situation changes dramatically. Now, when $\vec{E}^{AC} \parallel \vec{B}$, the resonance is seen, but for $\vec{E}^{AC} \perp \vec{B}$ no resonance can be detected. Thus, by rotating α by 45° we have rotated the amplitude dependence on Θ by the double angle,

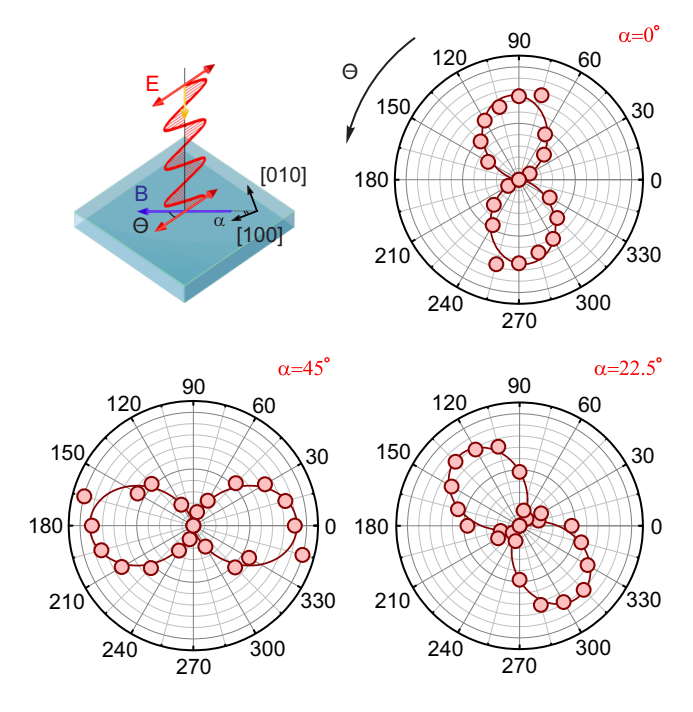


FIG. 4. Polar diagrams of the ESR resonance amplitude versus angle $\Theta = \angle \vec{B}, \vec{E}^{AC}$ between an external magnetic field and the electric field of the incident wave. Each diagram was measured for a fixed angle α between the external magnetic field and the [100] axis: $\alpha = 0^{\circ}$, 22.5°, and 45°, respectively. Points show the experimental data. Solid lines correspond to the theory, Eq. (3). The top left panel shows the orientation of the sample with respect to an incident THz wave and an external magnetic field. Note the double angle rotation of the excitation curve compared to the angle in the experiment.

 $2\alpha=90^\circ$. Indeed, in the intermediate case of $\alpha=22.5^\circ$, the polarization dependence shows the same shape as for $\alpha=0^\circ$, but it is rotated by 45° in Θ . Thus, turning the DC magnetic field \vec{B} from the crystallographic direction [100] by an angle α , we rotate the polarization dependence on Θ by the double angle 2α . Our experiments show that the resonant magnetic field does not depend on α , indicating the in-plane isotropy of the sample. However, for a magnetic dipole interaction, we would not expect the ESR signal to depend on the relative orientation of the static magnetic field and the crystal axes of the sample, which is in contrast to our observations.

Theory and discussion. Electron spin dynamics is controlled by real magnetic fields, both static and alternating, as well as by effective fields resulting from the spin-orbit coupling. All these contributions can be expressed in terms of the following Hamiltonian:

$$\mathcal{H} = \sum_{\alpha\beta} \frac{g_{\alpha\beta}}{2} \mu_B \sigma_\alpha B_\beta^{\text{eff}}, \quad \vec{B}^{\text{eff}} = \vec{B} + \vec{B}^{\text{AC}} + \vec{B}_{\vec{k}}^{\text{SO}}. \quad (1)$$

Here $g_{\alpha\beta}$ (α , $\beta=x$, y, z) are the Cartesian components of the g-factor tensor, $\mu_B=|e|\hbar/(2m_0c)$ is the Bohr magneton, σ_α are the 2×2 Pauli matrices representing the spin operator, and an effective magnetic field $B^{\rm eff}$ has contributions both from the real magnetic field $\vec{B}+\vec{B}^{\rm AC}$ and the wave vector \vec{k} -dependent effective field produced by the spin-orbit coupling, $\vec{B}_{7}^{\rm SO}$.

The symmetry analysis [32] shows that in the case of the symmetric heterostructure, the Z valley of AlAs quantum

well has D_{2d} point symmetry and the effective field can be expressed as

$$\vec{B}_{\vec{k}}^{\text{SO,BIA}} = \frac{2\beta}{\mu_B g_x} (-k_x, k_y, 0),$$
 (2)

where β is the parameter describing the bulk inversion asymmetry (Dresselhaus) term, and we recall that g_x is the in-plane component of the electron g-factor. In the presence of electromagnetic radiation, the components of the wavevector are replaced by $\vec{k} \to \vec{k} - (e/c\hbar)\vec{A}^{\rm AC}$ with the vector potential $\vec{A}^{\rm AC} = -\mathrm{i}(c/\omega)\vec{E}^{\rm AC}$.

Owing to the effective magnetic field induced by the spinorbit coupling, the ESR can be excited by an electric field component \vec{E}^{AC} of the electromagnetic wave [5].

Now we demonstrate that the Dresselhaus contribution is indeed responsible for the observed ESR both in the Faraday and Voigt geometries, while $\vec{B}^{\rm AC}$ and the Rashba structure-inversion asymmetry term described by $\vec{B}^{\rm SO}_{\vec{k}} \propto (k_y, -k_x, 0)$ are both irrelevant.

Indeed, the experiments in the Faraday geometry, Fig. 2, demonstrate that the ESR occurs for the CR inactive magnetic fields. For $g_z > 0$, it implies that the rotation of \vec{B}^{AC} that causes the CR and the rotation of \vec{B}^{eff} that causes the ESR should be in the opposite directions [32]. It is only possible for the spin-orbit magnetic field in the form of Eq. (2) that rotates in the opposite sense to the rotation of \vec{B}^{AC} and \vec{E}^{AC} of the THz wave.

Additional calculations show [32] that the dependence of ESR signal on the angles $\alpha = \angle \vec{B}$, [100] and $\Theta = \angle \vec{B}$, \vec{E}^{AC} in the Voigt geometry takes the form

$$I_{\rm ESR} \propto \sin^2(2\alpha - \Theta),$$
 (3)

fully in line with Figs. 3 and 4, demonstrating a characteristic dipolelike distribution reproducing the experimental dependence, Fig. 4.

For magnetodipole transitions where the ESR is excited via $\vec{B}^{\rm AC}$ and for Rashba-type (structure inversion asymmetry) spin-orbit coupling, $\vec{B}_{\vec{k}}^{\rm SO,SIA} \propto (k_y, -k_x, 0)$, the ESR intensity $I_{\rm ESR} \propto \cos^2 \Theta$, and is α independent.

The parameter describing the bulk inversion asymmetry β can be extracted from the experimental data. Theory [32] shows that the ratio of dips in the transmission for ESR and CR takes the form

$$\frac{\Delta T_{\rm ESR}}{\Delta T_{\rm CR}} = 2 \left(\frac{\beta}{\hbar c}\right)^2 \frac{m_c c^2}{\hbar \omega_L} \frac{\tau_s}{\tau_p} \left(\frac{\omega_L}{\omega_c + \omega_L}\right)^2,\tag{4}$$

where $\tau_s \approx 1.3$ ns and $\tau_p \approx 1.1$ ps are the relaxation times controlling the linewidths of ESR and CR in the Faraday geometry, respectively. The experiment gives $\beta \approx 7$ meVÅ, which agrees with the estimate from the spin-splitting enhancement [38]. Note, the magnitude of the effective magnetic field produced by \vec{E}^{AC} via the spin-orbit coupling, Eq. (2) $|\vec{B}^{SO,AC}| = 2\beta e/(\mu_B g_x \hbar \omega)|\vec{E}^{AC}|$, exceeds by far $|\vec{B}^{AC}|$, confirming a dominant role of the spin-orbit interaction in the ESR. Therefore, the interaction between spin and light should retain its electric dipole nature in a vast class of material systems with even stronger SOI, including both conventional epitaxial structures [39,40] and the van der Waals stacks [41–43].

In conclusion, we have studied the interaction between electromagnetic radiation and the spin ensemble of a two-dimensional electron system hosted in an AlAs quantum well. In the Faraday geometry, the spin resonance was observed exclusively when using circularly polarized electromagnetic waves in the polarity of the magnetic field that is normally inactive for cyclotron resonance. In the Voigt geometry, the amplitude of the spin resonance showed a strong dependence on the relative orientation of the incident electromagnetic wave with respect to the crystal axes of the sample and the static magnetic field. These findings reveal the mechanism of spin resonance excitation in this system. Through theoretical analysis, we have shown that the observed ESR is driven by the electric field component of the incident radiation and

results from the Dresselhaus spin-orbit interaction, originating from the bulk inversion asymmetry. Our results demonstrate not only that resolving the polarization dependencies of ESR in a 2DES is experimentally feasible but also that it is a powerful tool for identifying the underlying EDSR mechanism and reconstructing the spin-orbit coupling in these systems.

Acknowledgments. We are grateful to E. L. Ivchenko for valuable discussions. The authors acknowledge TU Wien Bibliothek for financial support through its Open Access Funding Program and the Russian Science Foundation (Grant No. 20-72-10097-extension). Theoretical analysis of M.M.G. was supported by the RSF Project No. 23-12-00142.

Data availability. The data that support the findings of this article are openly available [44]; embargo periods may apply.

- [1] F. Bloch, Nuclear induction, Phys. Rev. **70**, 460 (1946).
- [2] G. Dresselhaus, Spin-orbit coupling effects in zinc blende structures, Phys. Rev. 100, 580 (1955).
- [3] Yu. A. Bychkov and E. I. Rashba, Properties of a 2D electron gas with lifted spectral degeneracy, JETP Lett. **39**, 78 (1984).
- [4] E. L. Ivchenko, A. Yu. Kaminski, and U. Roössler, Heavylighthole mixing at zinc-blende (001) interfaces under normal incidence, Phys. Rev. B 54, 5852 (1996).
- [5] E. I. Rashba, Properties of semiconductors with an extremum loop. I. Cyclotron and combinational resonance in a magnetic field perpendicular to the plane of the loop, Sov. Phys. Solid State 2, 1109 (1960).
- [6] E. I. Rashba and V. I. Sheka, Electric-dipole spin resonances, in *Landau Level Spectroscopy*, edited by G. Landwehr and E. I. Rashba (North-Holland/Elsevier, Amsterdam, 1991), p. 131.
- [7] M. Duckheim and D. Loss, Electric-dipole-induced spin resonance in disordered semiconductors, Nat. Phys. 2, 195 (2006).
- [8] P. Stano and D. Loss, Review of performance metrics of spin qubits in gated semiconducting nanostructures, Nat. Rev. Phys. 4, 672 (2022).
- [9] J. W. G. van den Berg, S. Nadj-Perge, V. S. Pribiag, S. R. Plissard, E. P. A. M. Bakkers, S. M. Frolov, and L. P. Kouwenhoven, Fast spin-orbit qubit in an indium antimonide nanowire, Phys. Rev. Lett. 110, 066806 (2013).
- [10] M. Shafiei, K. C. Nowack, C. Reichl, W. Wegscheider, and L. M. K. Vandersypen, Resolving spin-orbit- and hyperfinemediated electric dipole spin resonance in a quantum dot, Phys. Rev. Lett. 110, 107601 (2013).
- [11] R. Li, J. Q. You, C. P. Sun, and F. Nori, Hybrid quantum circuits: Strong coupling between semiconductor qubits and microwave photons (spectroscopy/control of spin-orbit states), Phys. Rev. Lett. 111, 086805 (2013).
- [12] G. Scalari, C. Maissen, D. Turcinkova, D. Hagenmüller, S. De Liberato, C. Ciuti, C. Reichl, D. Schuh, W. Wegscheider, M. Beck, and J. Faist, Ultrastrong coupling of the cyclotron transition of a 2D electron gas to a THz metamaterial, Science 335, 1323 (2012).
- [13] A. Bayer, M. Pozimski, S. Schambeck, D. Schuh, R. Huber, D. Bougeard, and C. Lange, Nonlinear terahertz response of a two-dimensional electron gas in GaAs/AlGaAs heterostructures, Nano Lett. 17, 6340 (2017).

- [14] C. Schneider, M. M. Glazov, T. Korn, S. Höfling, and B. Urbaszek, Two-dimensional semiconductors in the regime of strong light-matter coupling, Nat. Commun. 9, 2695 (2018).
- [15] T. Weber, L. Kuehner, L. Sortino, A. B. Mhenni, N. P. Wilson, J. Kühne, J. J. Finley, S. A. Maier, and A. Tittl, Intrinsic strong light-matter coupling with self-hybridized bound states in the continuum in van der Waals metasurfaces, Nat. Mater. 22, 970 (2023).
- [16] R. L. Bell, Electric dipole spin transitions in InSb, Phys. Rev. Lett. 9, 52 (1962).
- [17] Y.-F. Chen, M. Dobrowolska, J. K. Furdyna, and S. Rodriguez, Interference of electric-dipole and magnetic-dipole interactions in conduction-electron-spin resonance in InSb, Phys. Rev. B 32, 890 (1985).
- [18] S. Gopalan, S. Rodriguez, J. Mycielski, A. Witowski, M. Grynberg, and A. Wittlin, Electric-dipole spin resonance in n-type Cd_{1-x}Mn_xSe, Phys. Rev. B 34, 5466 (1986).
- [19] R. Meisels, I. Kulac, F. Kuchar, and M. Kriechbaum, Electron spin resonance of the two-dimensional electron system in Al_xGa_{1-x}As/GaAs at subunity filling factors, Phys. Rev. B 61, 5637 (2000).
- [20] M. Schulte, J. G. S. Lok, G. Denninger, and W. Dietsche, Electron spin resonance on a two-dimensional electron gas in a single AlAs quantum well, Phys. Rev. Lett. 94, 137601 (2005).
- [21] Z. Wilamowski, H. Malissa, F. Schäffler, and W. Jantsch, g-factor tuning and manipulation of spins by an electric current, Phys. Rev. Lett. 98, 187203 (2007).
- [22] A. V. Stier, C. J. Meining, V. R. Whiteside, B. D. McCombe, E. I. Rashba, P. Grabs, and L. W. Molenkamp, Electric-dipole spin resonance and spin orbit coupling effects in odd-integer quantum Hall edge channels, Phys. Rev. B 107, 045301 (2023).
- [23] G. V. Kozlov and A. A. Volkov, Coherent source submillimeter wave spectroscopy, in *Millimeter and Submillimeter Wave Spectroscopy of Solids*, edited by G. Grüner (Springer, Berlin, 1998), p. 51.
- [24] M. Shayegan, E. P. De Poortere, O. Gunawan, Y. P. Shkolnikov, E. Tutuc, and K. Vakili, Two-dimensional electrons occupying multiple valleys in AlAs, Phys. Status Solidi B 243, 3629 (2006).
- [25] H. W. van Kesteren, E. C. Cosman, P. Dawson, K. J. Moore, and C. T. Foxon, Order of the *X* conduction-band valleys in type-II GaAs/AlAs quantum wells, Phys. Rev. B 39, 13426 (1989).

- [26] S. Yamada, K. Maezawa, W. T. Yuen, and R. A. Stradling, X-conduction-electron transport in very thin AlAs quantum wells, Phys. Rev. B **49**, 2189 (1994).
- [27] A. R. Khisameeva, A. V. Shchepetilnikov, V. M. Muravev, S. I. Gubarev, D. D. Frolov, Yu. A. Nefyodov, I. V. Kukushkin, C. Reichl, L. Tiemann, W. Dietsche, and W. Wegscheider, Direct observation of a Γ-X energy spectrum transition in narrow AlAs quantum wells, Phys. Rev. B 97, 115308 (2018).
- [28] A. R. Khisameeva, A. V. Shchepetilnikov, V. M. Muravev, S. I. Gubarev, D. D. Frolov, Yu. A. Nefyodov, I. V. Kukushkin, C. Reichl, W. Dietsche, and W. Wegscheider, Achieving balance of valley occupancy in narrow AlAs quantum wells, J. Appl. Phys. 125, 154501 (2019).
- [29] M. L. Savchenko, A. Shuvaev, I. A. Dmitriev, S. D. Ganichev, Z. D. Kvon, and A. Pimenov, Demonstration of high sensitivity of microwave-induced resistance oscillations to circular polarization, Phys. Rev. B 106, L161408 (2022).
- [30] V. Dziom, A. Shuvaev, A. Pimenov, G. V. Astakhov, C. Ames, K. Bendias, J. Böttcher, G. Tkachov, E. M. Hankiewicz, C. Brüne, H. Buhmann, and L. W. Molenkamp, Observation of the universal magnetoelectric effect in a 3D topological insulator, Nat. Commun. 8, 15197 (2017).
- [31] J. Gospodarič, A. Shuvaev, N. N. Mikhailov, Z. D. Kvon, E. G. Novik, and A. Pimenov, Energy spectrum of semimetallic HgTe quantum wells, Phys. Rev. B 104, 115307 (2021).
- [32] See Supplemental Material at https://link.aps.org/supplemental/10.1103/4lyv-jvq5 for detailed information. This includes references to S. S. Krishtopenko, V. I. Gavrilenko, M. Goiran, Exchange interaction effects in electron spin resonance: Larmor theorem violation in narrow gap quantum well heterostructures, J. Phys.: Condens. Matter 24, 252201 (2012); T. Ando, Theory of cyclotron resonance lineshape in a two-dimensional electron system, J. Phys. Soc. Japan 38, 989 (1975); M. M. Glazov, Magnetic field effects on spin relaxation in heterostructures, Phys. Rev. B 70, 195314 (2004); K. Vakili, Y. P. Shkolnikov, E. Tutuc, E. P. De Poortere, and M. Shayegan, Spin susceptibility of two-dimensional electrons in narrow AlAs quantum wells, Phys. Rev. Lett. 92, 226401 (2004).
- [33] A. V. Shchepetilnikov, Yu. A. Nefyodov, I. V. Kukushkin, L. Tiemann, C. Reichl, W. Dietsche, and W. Wegscheider, Electron g-factor anisotropy in an AlAs quantum well probed by ESR, Phys. Rev. B 92, 161301(R) (2015).

- [34] D. Fukuoka, K. Oto, K. Muro, Y. Hirayama, and N. Kumada, Skyrmion effect on the relaxation of spin waves in a quantum Hall ferromagnet, Phys. Rev. Lett. **105**, 126802 (2010).
- [35] S. Dickmann and T. Ziman, Competing hyperfine and spinorbit couplings: Spin relaxation in a quantum Hall ferromagnet, Phys. Rev. B 85, 045318 (2012).
- [36] A. S. Zhuravlev, S. Dickmann, L. V. Kulik, and I. V. Kukushkin, Slow spin relaxation in a quantum Hall ferromagnet state, Phys. Rev. B 89, 161301(R) (2014).
- [37] A. V. Shchepetilnikov, A. R. Khisameeva, Yu. A. Nefyodov, and I. V. Kukushkin, Spin relaxation in a strongly correlated quantum Hall ferromagnet, Phys. Rev. B 103, 195313 (2021).
- [38] A. V. Shchepetilnikov, D. D. Frolov, Yu. A. Nefyodov, I. V. Kukushkin, L. Tiemann, C. Reichl, W. Dietsche, and W. Wegscheider, Spin-orbit coupling effects in the quantum Hall regime probed by electron spin resonance, Phys. Rev. B 98, 241302(R) (2018).
- [39] A. J. A. Beukman, F. K. de Vries, J. van Veen, R. Skolasinski, M. Wimmer, F. Qu, D. T. de Vries, B.-M. Nguyen, W. Yi, A. A. Kiselev, M. Sokolich, M. J. Manfra, F. Nichele, C. M. Marcus, and L. P. Kouwenhoven, Spin-orbit interaction in a dual gated InAs/GaSb quantum well, Phys. Rev. B 96, 241401(R) (2017).
- [40] F. Fan, Y. Chen, D. Pan, J. Zhao, and H. Q. Xu, Measurements of spin-orbit interaction in epitaxially grown InAs nanosheets, Appl. Phys. Lett. 117, 132101 (2020).
- [41] N. Alidoust, G. Bian, S.-Y. Xu, R. Sankar, M. Neupane, C. Liu, I. Belopolski, D.-X. Qu, J. D. Denlinger, F.-C. Chou, and M. Z. Hasan, Observation of monolayer valence band spin-orbit effect and induced quantum well states in MoX₂, Nat. Commun. 5, 4673 (2014).
- [42] Z. Wang, D.-K. Ki, J. Y. Khoo, D. Mauro, H. Berger, L. S. Levitov, and A. F. Morpurgo, Origin and magnitude of 'designer' spin-orbit interaction in graphene on semiconducting transition metal dichalcogenides, Phys. Rev. X 6, 041020 (2016).
- [43] T. Wang, M. Vila, M. P. Zaletel, and S. Chatterjee, Electrical control of spin and valley in spin-orbit coupled graphene multilayers, Phys. Rev. Lett. 132, 116504 (2024).
- [44] D. Khudaiberdiev, Original data for "Polarization resolved electron spin resonance in a two-dimensional electron system" (1.0.0) (data set). TU Wien, https://doi.org/10.48436/b27m5-0zz56.